Effect of porosity in interfacial stress analysis of perfect FGM beams reinforced with a porous functionally graded materials plate

Benferhat Rabia[1,2], Tahar Hassaine Daouadji[*1,2] and Rabahi Abderezak[1,2]

[1]*Département de génie civil, Université Ibn Khaldoun Tiaret, BP 78 Zaaroura, Tiaret, Algérie*
[2]*Laboratoire de Géomatique et Développement Durable, Université de Tiaret, Algérie*

Abstract.   In this paper, a general model is developed to predict the distribution of interfacial shear and normal stresses of FG beam reinforced by porous FGM plates under mechanical loading. The beam is assumed to be isotropic with a constant Poisson's ratio and power law elastic modulus through the beam thickness. Stress distributions, depending on an inhomogeneity constant, were calculated and presented in graphicals forms. It is shown that both the normal and shear stresses at the interface are influenced by the material and geometry parameters of the composite beam, and it is shown that the inhomogeneities play an important role in the distribution of interfacial stresses. The results presented in the paper can serve as a benchmark for future analyses of functionally graded beams strengthened by imperfect varying properties plates. Numerical comparisons between the existing solutions and the present new solution enable a clear appreciation of the effects of various parameters. The results of this study indicated that the imperfect functionally graded panel strengthening systems are effective in enhancing flexural behavior of the strengthened FGM beams. This research is helpful in understanding the mechanical behaviour of the interface and design of hybrid structures.

Keywords: interfacial stresses; FG beam; strengthening imperfect plate; functionally graded material

1. Introduction

The technique of rehabilitating and strengthening conventional reinforced concrete beams with externally bonded fiber reinforced composite laminates has shown great promise as a means for remedying structural deficiencies and enhancing the performance of civil engineering structures (Tounsi 2006, Hassaine Daouadji *et al.* 2017 and Benyoucef *et al.* 2006). As a result, various experimental investigations of this strengthening technique have recently been conducted. The main goals of these studies were either to evaluate the effectiveness of the composite reinforcement on the flexural performance of concrete beams (Tounsi *et al.* 2008, Benferhat *et al.* 2018, Bouakaz *et al.* 2014, Tahar *et al.* 2016, El Mahi *et al.* 2014, Guenaneche *et al.* 2014, Adim *et al.* 2016, Krour *et al.* 2014 and Rabahi *et al.* 2015) or to assess the influence of various factors on the possible failure modes (Shen *et al.* 2001, Smith *et al.* 2001, Yang *et al.* 2007,Hassaine Daouadji 2013, Chaded 2018, Benhenni2018a, Benhenni 2018b, Rabahi 2018, Bensatallah 2018, Tayeb 2019, Benferhat 2019, Benhenni 2019, Hassaine Daouadji 2012, Tahar 2013, Abdelhak 2015, Khalifa 2016, Rabahi 2019, Benferhat 2015, Tahar 2015 and El Amrani *et al.* 2006). A review of more recent progress in the field of composites for structural strengthening and repair can be found in the survey article by Tounsi *et al.* (2006). Analysis of interfacial shear stress in beams with bonded composite plates has been performed by several researchers (Jian *et al.* 2007, Yang *et al.* 2010, Abderezak *et al.* 2015 and Touati *et al.* 2015). The analysis provided closed-form formulas for the calculation of interfacial shear and peeling stress in beams with bonded non-prestressed plates or laminates. Mohammadimehr *et al.* 2017 studied the buckling, and free vibration analysis of tapered functionally graded carbon nanotube reinforced composite (FG-CNTRC) micro Reddy beam under longitudinal magnetic field using finite element method (FEM). Farajpour *et al.* 2016 developed a new size-dependent plate model is developed based on the higher-order nonlocal strain gradient theory. Mohammadimehr *et al.* 2018 presented static, buckling and free vibration analyses of a sinusoidal micro composite beam reinforced by single-walled carbon nanotubes (SWCNTs) with considering temperature-dependent material properties embedded in an elastic medium in the presence of magnetic field under transverse uniform load. Ghorbanpour *et al.* 2017 studied the vibration and instability of axially moving viscoelastic micro-plate using Sinusoidal shear deformation theory (SSDT). Arani *et al.* 2012 studied the stress analysis of a long piezoelectric polymeric hollow cylinder reinforced with carbon nanotube (CNT) under combined magneto-thermo-electro-mechanical loading. Mohammadimehr *et al.* 2017 presented the size-dependent effect on free vibration of double-bonded isotropic piezoelectric Timoshenko microbeams using strain gradient and surface stress elasticity theories under initial stress.

However, the problem of interfacial stress when laminates are used in strengthening and repair has treated (Zidani *et al.* 2015, Tounsi *et al.* 2008 and Tahar *et al.* 2013). In this investigation, only interfacial shear stress was studied and the analyzed beam was not loaded.

∗Corresponding author, Professor.
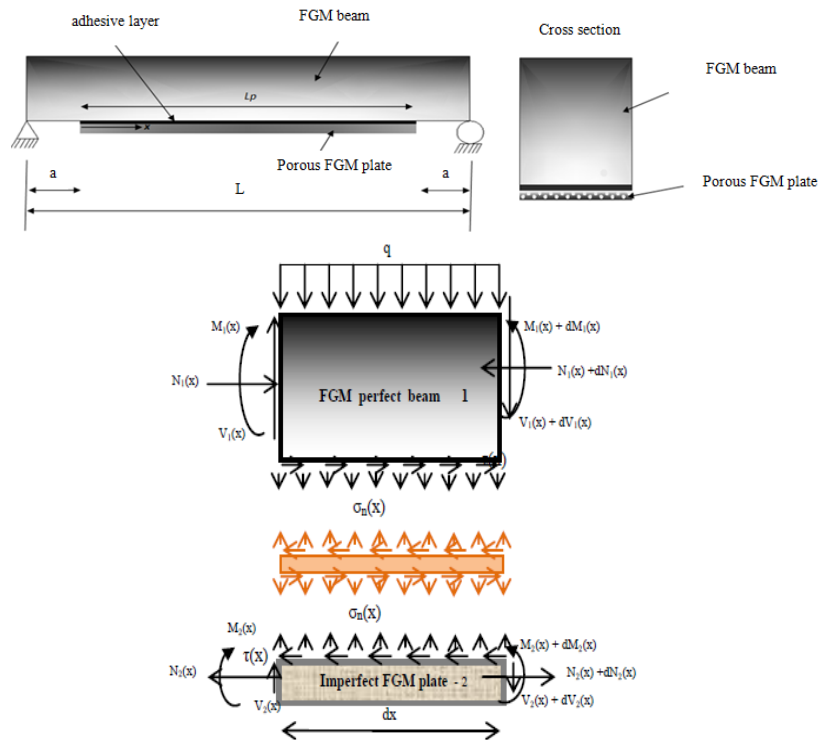 E-mail: daouadjitahar@gmail.com

Fig. 1 Simply supported beam strengthened bonded with imperfect FGM plate

During the process of sintering of FGM materials, due to big difference in solidification between the material constituents, however, porosities or micro voids through material can happen regularly (Zhu *et al.* 2001). A thorough research has been done on porosities occurring inside FGM samples manufactured by a multistep sequential infiltration technique (Wattanasakulpong *et al.* 2012). Porosity maybe change the elastic and mechanical properties. To the authors' knowledge, no researchers have given much attention to the effect of the porosity on the interfacial stresses. Based on this information about porosities in FGMs, it is important to consider the porosity effect and its distribution shape on the interfacial stresses.

The objective of this study is to develop a procedure that predicts the shear and normal stresses in the interface between the perfect FG beam and the repairing porous FGM plate with reasonable accuracy. The material properties of the functionally graded beams are assumed to vary continuously through the thickness of the beam, according to the power law distribution law. A parametric study was carried out to show the effects of some design variables, e.g., thickness of adhesive layer, thickness of the bonded plate. The effects of the material and geometry parameters on the interface stresses are considered and compared with that resulting from literature. Finally, some concluding remarks are summarized in conclusion. It is believed that the present results will be of interest to civil and structural engineers and researchers.

2. Method of solution

2.1 Assumptions

The present analysis takes into consideration the transverse shear stress and strain in the beam and the plate but ignores the transverse normal stress in them. One of the analytical approach proposed by Benferhat *et al.* (2018) for FGM perfect beam strengthened with a bonded imperfect FGM Plate (Fig 1) was used in order to compare it with another analytical models.

The analytical approach (Benferhat *et al.* 2018) is based on the following assumptions:

- Elastic stress strain relationship for FGM and adhesive;
- There is a perfect bond between the imperfect FGM plate and the beam;
- The adhesive is assumed to only play a role in transferring the stresses from the FGM beam to the composite plate reinforcement;
- The stresses in the adhesive layer do not change through the direction of the thickness.

Since the functionally graded materials is an orthotropic material. In analytical study (Benferhat *et al.* 2018), the classical plate theory is used to determine the stress and strain behaviors of the externally bonded imperfect FGM plate in order to investigate the whole mechanical performance of the composite – strengthened structure.

2.2. Properties of the FGM constituent materials

In this study, we consider an imperfect FGM plate with a volume fraction of porosity α ($\alpha < 1$), with different form of distribution between the metal and the ceramic. The modified mixture rule proposed by Wattanasakulpong and Ungbhakorn 2014, Adim *et al.* 2016, Abualnour *et al.* 2018, Draiche *et al.* 2016, Kaci *et al.* 2018, Bakhadra *et al.* 2018, Bouhadra *et al.* 2018, Ait Atman *et al.* 2015, Benferhat *et al.* 2016, Belabed *et al.* 2018, Bellifa *et al.* 2017, Bouadi *et al.* 2018, Hassaine Daouadji *et al.* 2016 and Khalifa *et al.*

Table 1 Deferent distribution forms of porosity

Distribution forms of Porosity	Elastic Modulus Expression	
Uniform distribution shape of the porosity	$E_2 = (e_c - e_m) * ((\frac{z}{t_2} + 0.5))^k + e_m - (e_c + e_m) * \frac{\alpha}{2}$	(3)
Form "X" distribution shape of the porosity	$E_2 = (e_c - e_m) * ((\frac{z}{t_2} + 0.5))^k + e_m - (e_c + e_m) * \frac{\alpha}{2} * (2 * \frac{z}{t_2})$	(4)
Form " O " distribution shape of the porosity	$E_2 = (e_c - e_m) * ((\frac{z}{t_2} + 0.5))^k + e_m - (e_c + e_m) * \frac{\alpha}{2} * (1 - 2 * \frac{|z|}{t_2})$	(5)
Inverted Form "V" distribution shape of the porosity	$E_2 = (e_c - e_m) * ((\frac{z}{t_2} + 0.5))^k + e_m - (e_c + e_m) * \frac{\alpha}{2} * (\frac{1}{2} - \frac{z}{t_2})$	(6)
Form "V" distribution shape of the porosity	$E_2 = (e_c - e_m) * ((\frac{z}{t_2} + 0.5))^k + e_m - (e_c + e_m) * \frac{\alpha}{2} * (\frac{1}{2} + \frac{z}{t_2})$	(7)

2018, is

$$P = P_m (V_m - \frac{\alpha}{2}) + P_c ((\frac{z}{h} + \frac{1}{2})^k - \frac{\alpha}{2}) \quad (1)$$

The modified mixture rule becomes

$$P = (P_c - P_m)(\frac{z}{h} + \frac{1}{2})^k + P_m - (P_c + P_m)\frac{\alpha}{2} \quad (2)$$

Where, k is the power law index that takes values greater than or equals to zero. The FGM plate becomes a fully ceramic plate when k is set to zero and fully metal for large value of k.

The Young's modulus (E) of the imperfect FG plate can be written as a functions of thickness coordinate, Z (middle surface). The material properties of a perfect FGM plate can be obtained when the volume fraction of porosity α is set to zero. Due to the small variations of the Poisson ratio ν, it is assumed to be constant. Several forms of porosity have been studied in the present work, such as "O", "V" and X", as follows (Table 1).

Equation 3 in table 1, which describes a uniform distribution of porosity, was extracted in the work of (Wattanasakulpong *et al.* 2014). On the other hand, the other equations (4, 5, 6 and 7) that describe the other distributions forms are proposed by us, where the rule of mixture has been reformulated to evaluate characteristics of materials having different distribution shapes of porosity.

The linear constitutive relations of a FG plate can be written as

$$\begin{Bmatrix} \sigma_x \\ \sigma_y \\ \tau_{yz} \\ \tau_{xz} \\ \tau_{xy} \end{Bmatrix} = \begin{bmatrix} \frac{E(z)}{1-\nu^2} & \frac{\nu E(z)}{1-\nu^2} & 0 & 0 & 0 \\ \frac{\nu E(z)}{1-\nu^2} & \frac{E(z)}{1-\nu^2} & 0 & 0 & 0 \\ 0 & 0 & \frac{E(z)}{2(1+\nu)} & 0 & 0 \\ 0 & 0 & 0 & \frac{E(z)}{2(1+\nu)} & 0 \\ 0 & 0 & 0 & 0 & \frac{E(z)}{2(1+\nu)} \end{bmatrix} \begin{Bmatrix} \varepsilon_x \\ \varepsilon_y \\ \gamma_{yz} \\ \gamma_{xz} \\ \gamma_{xy} \end{Bmatrix} \quad (8)$$

where $(\sigma_x, \sigma_y, \tau_{xy}, \tau_{yz}, \tau_{xz})$ and $(\varepsilon_x, \varepsilon_y, \gamma_{xy}, \gamma_{yz}, \gamma_{xz})$ are the stress and strain components, respectively , and A_{ij}, D_{ij} are the plate stiffness, defined by:

$$A_{ij} = \int_{-h/2}^{h/2} Q_{ij} dz \qquad D_{ij} = \int_{-h/2}^{h/2} Q_{ij} z^2 dz \quad (9)$$

where A'_{11}, D'_{11} are defined as

$$A_{11}^{'} = \frac{A_{22}}{A_{11}A_{22} - A_{12}^2} \qquad D_{11}^{'} = \frac{D_{22}}{D_{11}D_{22} - D_{12}^2} \quad (10)$$

2.3 Shear stress distribution along the reinforced beam

The governing differential equation for the interfacial shear stress is expressed as (Benferhat 2018)

$$\frac{d^2\tau(x)}{dx^2} - \frac{1}{\frac{t_a}{G_a} + \frac{t_1}{4G_1}} \left(A_{11}^{'} + \frac{b_2}{E_1 A_1} + \frac{(y_1 + t_2/2)(y_1 + t_a + t_2/2)}{E_1 I_1 D_{11}^{'} + b_2} b_2 D_{11}^{'} \right) \tau(x)$$
$$+ \frac{1}{\frac{t_a}{G_a} + \frac{t_1}{4G_1}} \left(\frac{(y_1 + t_2/2)}{E_1 I_1 D_{11}^{'} + b_2} D_{11}^{'} \right) V_T(x) = 0 \quad (11)$$

where E_1 is the elastic modulus of the beam. G_1 is the transverse shear moduli of adherents 1. t_1 and t_2 are the thickness of adherends 1 and 2, respectively.

G_a and t_a are shear modulus and thickness of the adhesive, respectively. b_2 is the width of the reinforcing plate and y_1 the distance from the bottom of adherent 1 to its centroid.

$[A']$ is the inverse of the extensional matrix $[A]$ and $[D']$ is the inverse of the flexural matrix $[D]$.

For simplicity, the general solutions presented below are limited to loading which is either concentrated or uniformly distributed over part or the whole span of the beam, or both. For such loading, $d^2VT(x)/dx^2 = 0$, and the general solution to Eq. (11) is given by

$$\tau(x) = J_1 \cosh(\xi x) + J_2 \sinh(\xi x) + \frac{1}{(\frac{t_a}{G_a} + \frac{t_1}{4G_1})\xi^2} (\frac{y_1 + \frac{t_2}{2}}{E_1 I_1 D_{11}^{'} + b_2} D_{11}^{'}) V_T(x) \quad (12)$$

Where

$$\xi^2 = \frac{1}{\frac{t_a}{G_a} + \frac{t_1}{4G_1}} \left(A_{11}^{'} + \frac{b_2}{E_1 A_1} + \frac{(y_1 + t_2/2)(y_1 + t_a + t_2/2)}{E_1 I_1 D_{11}^{'} + b_2} b_2 D_{11}^{'} \right) \quad (13)$$

And J_1 and J_2 are constant coefficients determined from the boundary conditions. In the present study, a simply supported beam has been investigated which is subjected to a uniformly distributed load (Fig 1). The interfacial shear stress for this uniformly distributed load at any point is written as [5]

$$\tau(x) = \left[\frac{\frac{K_1 y_1}{E_1 I_1}}{2} a (L-a) - \frac{1}{(\frac{t_a}{G_a} + \frac{t_1}{4G_1})\xi^2} (\frac{y_1 + \frac{t_2}{2}}{E_1 I_1 D_{11}^{'} + b_2} D_{11}^{'}) \right] \frac{q e^{-\xi x}}{\xi} + \frac{1}{(\frac{t_a}{G_a} + \frac{t_1}{4G_1})\xi^2} (\frac{y_1 + \frac{t_2}{2}}{E_1 I_1 D_{11}^{'} + b_2} D_{11}^{'}) q(\frac{L}{2} - a - x) \quad (14)$$
$$0 \le x \le L_P$$

Where q is the uniformly distributed load and x; a; L and Lp are defined in Fig. 1.

2.4 Normal stress distribution along the reinforced beam

The following governing differential equation for the interfacial normal stress (Benferhat *et al.* 2018)

$$\frac{d^4\sigma_n(x)}{dx^4} + K_n\left(D'_{11} + \frac{b_2}{E_1 I_1}\right)\sigma_n(x) - K_n\left(D'_{11}\frac{t_2}{2} - \frac{y_1 b_2}{E_1 I_1}\right)\frac{d\tau(x)}{dx} + \frac{qK_n}{E_1 I_1} = 0 \quad (15)$$

where K_n is the normal stiffness of the adhesive per unit length.

The general solution to this fourth–order differential equation is

$$\sigma_n(x) = e^{-\delta x}[J_3\cos(\delta x) + J_4\sin(\delta x)] + e^{\delta x}[J_5\cos(\delta x) + J_6\sin(\delta x)] - \left(\frac{y_1 b_2 - \frac{D'_{11}E_1 I_1 t_2}{2}}{D'_{11}E_1 I_1 + b_2}\right)\frac{d\tau(x)}{dx} - \frac{1}{D'_{11}E_1 I_1 + b_2}q \quad (16)$$

For large values of x it is assumed that the normal stress approaches zero and, as a result, $J_5 = J_6 = 0$. The general solution therefore becomes

$$\sigma_n(x) = e^{-\delta x}[J_3\cos(\delta x) + J_4\sin(\delta x)] - \left(\frac{y_1 b_2 - \frac{D'_{11}E_1 I_1 t_2}{2}}{D'_{11}E_1 I_1 + b_2}\right)\frac{d\tau(x)}{dx} - \frac{1}{D'_{11}E_1 I_1 + b_2}q \quad (17)$$

Where

$$\delta = \sqrt[4]{\frac{K_n}{4}\left(D'_{11} + \frac{b_2}{E_1 I_1}\right)} \quad (18)$$

As is described by Benferhat *et al.* (2018) , the constants J_3 and J_4 in Eq.(16) are determined using the appropriate boundary conditions and they are written as follows

$$J_3 = \frac{K_n\left[V_T(0) + \sqrt[4]{\frac{K_n}{4}(D'_{11} + \frac{b_2}{E_1 I_1})}M_T(0)\right]}{2\left[\sqrt[4]{\frac{K_n}{4}(D'_{11} + \frac{b_2}{E_1 I_1})}\right]^3 E_1 I_1} - \frac{b_2 K_n(\frac{y_1}{E_1 I_1} - \frac{D'_{11}t_2}{2b_2})}{2\left[\sqrt[4]{\frac{K_n}{4}(D'_{11} + \frac{b_2}{E_1 I_1})}\right]^3}\tau(0)$$
$$+ \frac{r_1\left[\frac{d^4\tau(0)}{dx^4} + \sqrt[4]{\frac{K_n}{4}(D'_{11} + \frac{b_2}{E_1 I_1})}\frac{d^3\tau(0)}{dx^3}\right]}{2\left[\sqrt[4]{\frac{K_n}{4}(D'_{11} + \frac{b_2}{E_1 I_1})}\right]^3} \quad (19)$$

$$J_4 = -\frac{K_n}{2\sqrt{\frac{K_n}{4}(D'_{11} + \frac{b_2}{E_1 I_1})}.E_1 I_1}M_T(0) - \frac{y_1 b_2 - \frac{D'_{11}E_1 I_1 t_2}{2}}{D'_{11}E_1 I_1 + b_2}\frac{d^3\tau(0)}{dx^3} \quad (20)$$

The above expressions for the constants J_3 and J_4 has been left in terms of the bending moment $M_T(0)$ and shear force $V_T(0)$ at the end of the soffit plate. With the constants J_3 and J_4 determined, the interfacial normal stress can then be found using Eq.(15).

3. Results: Discussion and analysis

In this section, we present numerical and graphical results to examine the effect of the porosity distribution form as well as other parameters that govern the stress distribution at the beam interface and the FGM reinforcement plate. Loading is always considered uniformly distributed and the properties of the materials (table 2) supported in this analysis are as follows

Table 2 Geometric and mechanical properties of the materials used

Materials	E GPa	Width (mm)	Thickness (mm)
Al₂O₃	380	b_1=200	
ZrO₂	151	b_1=200	
Al	70	b_1=200	Beam : Height t_1=300 mm
Ti-6Al-4V	105.7	b_1=200	Reinforcement plate: Thickness t_2=4mm
Aluminium oxide	320.2	b_1=200	
CFRP	100	b_2=200	
Adhesive	3	b_a=200	Adhesive layer : Thickness t_a=2

Table 3 Comparison of the maximum values of the interfacial stresses of a homogenous and non-homogenous beam.

Model	$\tau(x)$	$\sigma_n(x)$
Homogenous beam. k = 0		
Brairi-Analytical model (2018)	2.74	1.42
Brairi-FE model (2018)	2.8	1.6
Present Analytical model	2.75689	1.49672
Non-homogenous beam. k ≠ 0		
Brairi-Analytical model (2018)	0.31	0.16
Brairi-FE model (2018)	0.45	0.22
Present Analytical model	0.32244	0.19829

Table 3 show the comparison study of the maximum values of the interfacial stresses of a homogenous and non-homogenous FG beam reinforced with CFRP plate. From this table it can be seen that the results of the present method are closer to those obtained by FE models of Brairi *et al.* (2018) than its analytical model.

After the validation of the present method in Table 3, a parametric study will be conducted to present the effect of several parameters (different types of FGM plate combinations and different forms of porosity) on the interfacial stresses in the tables 4, 5 and 6. The present results will provide a useful reference for evaluating other analytical and numerical methods.

Table 4 present the results of the interface stresses of a FGM beam Al/Al₂O₃ and Ti-6Al-4V/ Al₂O₃. Different types of combination of the FGM reinforcing plate have been considered namely, FGM plate in: Al/Al₂O₃, Al/ZrO₂ and Ti-6Al-4V/ Al₂O₃. From these tables, it can be seen that the normal and shear stresses become lower when the reinforcement plate is Al/ZrO₂. This is expected because the Al/ZrO₂ plate is the one with the lowest stiffness.

Table 5 show the effect of porosity on the interfacial stresses of a FGM beam in Al/Al₂O₃ and Ti-6Al-4V/Al₂O₃ . The volume fraction of porosity is taken equal to (0.1, 0.15 and 0.2). The load is considered uniformly distributed. The power index is taken as 10 for the FGM reinforcement plate. It should be noted that normal and shear stresses become lower as the volume fraction of porosity in the reinforcement plate increases. It can also be noted that the interface stresses are lower when the FGM beam is Ti-6Al-

Table 4 Interface stresses of reinforced FGM beam by external bonding of different types of FGM plate combinations

Al/Al$_2$O$_3$ reinforced FGM beam by external bonding of different types of FGM plate combinations

FGM beam	Al/Al$_2$O$_3$ - k=10		Al/ZrO$_2$ - k=10		Ti-6Al-4V/Al$_2$O$_3$ - k=10	
	$\tau(x)$	$\sigma_n(x)$	$\tau(x)$	$\sigma_n(x)$	$\tau(x)$	$\sigma_n(x)$
Ceramic beam (k=0)	0.20419	0.13319	0.094585	0.083686	0.25101	0.15058
FGM beam (k=5)	0.40216	0.40216	0.19963	0.18106	0.78997	0.48994
FGM beam (k=10)	0.50731	0.33520	0.29171	0.26944	0.91193	0.56916
Aluminium beam (k=∞)	0.77572	0.52185	0.35594	0.33245	0.92081	0.57496

Ti-6Al-4V/Al$_2$O$_3$ reinforced FGM beam by external bonding of different types of FGM plate combinations

FGM beam	Al/Al$_2$O$_3$ - k=10		Al/ZrO$_2$ - k=10		Ti-6Al-4V/Al$_2$O$_3$ - k=10	
	$\tau(x)$	$\sigma_n(x)$	$\tau(x)$	$\sigma_n(x)$	$\tau(x)$	$\sigma_n(x)$
Ceramic beam (k=0)	0.23663	0.15481	0.23235	0.15318	0.29075	0.17491
FGM beam (k=5)	0.50053	0.33483	0.52203	0.35268	0.64058	0.39399
FGM beam (k=10)	0.55992	0.37622	0.55494	0.37584	0.69035	0.42582
Aluminium beam (k=∞)	0.56676	0.38100	0.55665	0.37706	0.69371	0.42797

Table 5 Porosity effect on the interface stresses of FGM beam reinforced by external bonding of FGM plate (Al/Al2O3) and subjected to uniformly distributed loading

Al/Al$_2$O$_3$ FGM reinforcement plate

Al/Al$_2$O$_3$ FGM beam	a=0.1		a=0.15		a=0.2	
	$\tau(x)$	$\sigma_n(x)$	$\tau(x)$	$\sigma_n(x)$	$\tau(x)$	$\sigma_n(x)$
Al/Al$_2$O$_3$ FGM beam (k=5)	0.46937	0.33969	0.40148	0.30231	0.33722	0.22998
Al/Al$_2$O$_3$ FGM beam (k=10)	0.60710	0.47742	0.53799	0.41063	0.47373	0.34637

Ti-6Al-4V/Al$_2$O$_3$ FGM reinforcement plate

Al/Al$_2$O$_3$ FGM beam	$\tau(x)$	$\sigma_n(x)$	$\tau(x)$	$\sigma_n(x)$	$\tau(x)$	$\sigma_n(x)$
Al/Al$_2$O$_3$ FGM beam (k=5)	0.40407	0.29062	0.35338	0.26470	0.30776	0.23817
Al/Al$_2$O$_3$ FGM beam (k=10)	0.46497	0.33636	0.41588	0.31364	0.37375	0.29159

Table 6 Effect of the porosity distribution form on the interface constraints of FGM beam reinforced by external bonding of FGM plate and subjected to a uniformly distributed loading

Effect of the porosity distribution form on the interface constraints of an Al/Al$_2$O$_3$ FGM beam reinforced by external bonding of FGM plate and subjected to a uniformly distributed loading

	Porosity distribution form	a=0.1		a=0.15		a=0.2	
		$\tau(x)$	$\sigma_n(x)$	$\tau(x)$	$\sigma_n(x)$	$\tau(x)$	$\sigma_n(x)$
Al/Al$_2$O$_3$ FGM plate k=5	Uniform form	0.81176	0.51908	0.78065	0.50157	0.75520	0.48190
	'O' form	0.84842	0.53210	0.84111	0.52312	0.84152	0.51244
	'X' form	0.87270	0.54066	0.86315	0.53093	0.84786	0.51460
	'V' form	0.84271	0.53016	0.82289	0.51680	0.80285	0.49904
	'V' form reversed	0.87808	0.54247	0.88050	0.53687	0.88458	0.52707
Al/Al$_2$O$_3$ FGM plate k=10	Uniform form	0.60710	0.44456	0.53799	0.41063	0.47373	0.37373
	'O' form	0.64875	0.46188	0.61449	0.44342	0.59579	0.42688
	'X' form	0.69656	0.48108	0.66613	0.46441	0.62439	0.43850
	'V' form	0.65328	0.46378	0.60519	0.43954	0.55376	0.40912
	'V' form reversed	0.69238	0.47944	0.67465	0.46782	0.66225	0.45356

Effect of the porosity distribution form on the interface constraints of an Ti-6Al-4V/ Al$_2$O$_3$ FGM beam reinforced by external bonding of FGM plate and subjected to a uniformly distributed loading

	Porosity distribution form	a=0.1		a=0.15		a=0.2	
		$\tau(x)$	$\sigma_n(x)$	$\tau(x)$	$\sigma_n(x)$	$\tau(x)$	$\sigma_n(x)$
Al/Al$_2$O$_3$ FGM plate k=5	Uniform form	0.63091	0.39917	0.61399	0.39058	0.60653	0.38359
	'O' form	0.65979	0.40949	0.66222	0.40796	0.67677	0.40860
	'X' form	0.67895	0.41631	0.67974	0.41412	0.68187	0.41031
	'V' form	0.65529	0.40793	0.64767	0.40280	0.64523	0.39756
	'V' form reversed	0.68326	0.41778	0.69366	0.41889	0.71178	0.42051
Al/Al$_2$O$_3$ FGM plate k=10	Uniform form	0.46497	0.33636	0.41588	0.31364	0.37375	0.29159
	'O' form	0.49716	0.34974	0.47546	0.33915	0.47070	0.33377
	'X' form	0.53419	0.36462	0.51574	0.35553	0.49344	0.34300
	'V' form	0.50062	0.35116	0.46820	0.33609	0.43729	0.31967
	'V' form reversed	0.53087	0.36334	0.52244	0.35824	0.52358	0.35500

4V /Al$_2$O$_3$ (the interfacial stresses become weaker when the reinforcement plate has a lower stiffness and when the FG beam has a highest stiffness). The effect of the porosity distribution form on the interfacial constraints of a Al/Al$_2$O$_3$ and Ti-6Al-4V/Al$_2$O$_3$ FGM beam is shown in table 6. The reinforcing FGM plate is considered Al/Al$_2$O$_3$. Various forms of porosity distribution in the reinforcing plate have been considered, namely, a uniform distribution, 'O', 'X', 'V'

and 'V' reversed. It can be concluded that the normal and shear stresses are lower when the porosity distribution in the reinforcement plate is uniform and when the combination of the reinforcing FGM plate is made of Ti-6Al-4V/ Al$_2$O$_3$.

Figures 2, 3, 4 and 5 show the variation of the normal stresses and shears as a function of the power index k of a FGM beam in Al / Al$_2$O$_3$ and Ti-6Al-4V/ Aluminum Oxide ,
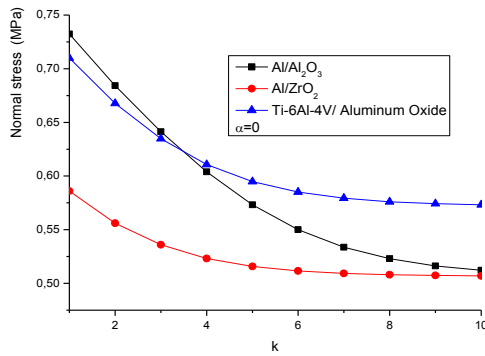
Fig. 2 Variation of the normal stress of a FGM beam in Al/Al$_2$O$_3$ reinforced in flexion with a porous varying properties plate under a uniformly distributed loading
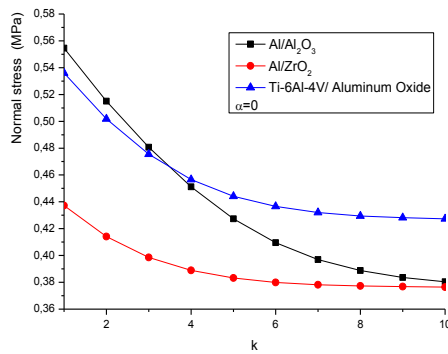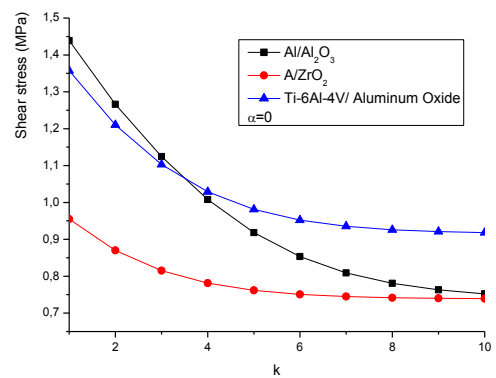

Fig. 4 Variation of the shear stress of a FGM beam in Al/Al$_2$O$_3$ reinforced in flexion with a porous varying properties plate under a uniformly distributed loading

Fig. 3 Variation of the normal stress of a FGM beam in Ti-6Al-4V/Aluminum oxyde reinforced in flexion with a porous varying properties plate under a uniformly distributed loading
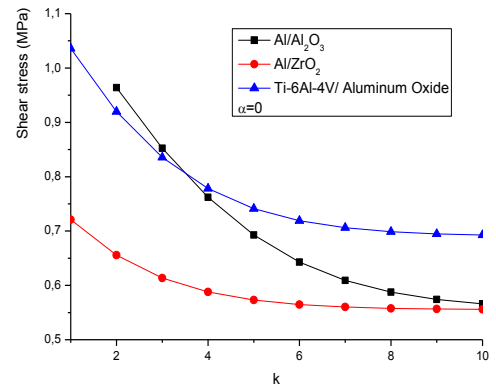

Fig. 5 Variation of the shear stress of a FGM beam in Ti-6Al-4V/Aluminum Oxide reinforced in flexion with a porous varying properties plate under a uniformly distributed loading
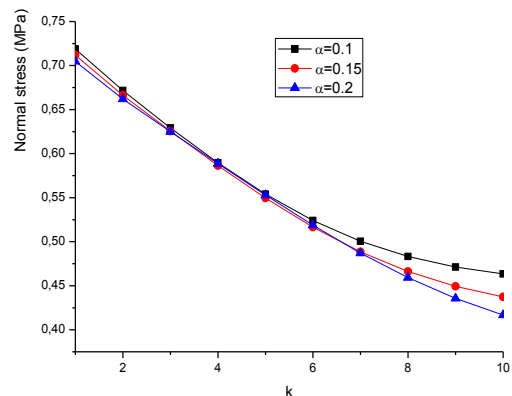
respectively. The beam is reinforced with different combinations of the reinforcing plate FGM. The volume fraction of porosity is taken equal to 0 (perfect reinforcing plate). From these figures it can be seen that the normal and shear stresses become lower with the increase of the power index k in the reinforcing plate FGM. It can also be noted that the interface stresses are lower when the reinforcing plate FGM is Al / ZrO$_2$. The interfacial stresses are higher when k < 3.5 because the Al / Al$_2$O$_3$ reinforcement plate becomes richer in ceramics Al$_2$O$_3$ (higher stiffness: E$_{Al2O3}$ > E$_{Aluminum\ oxide}$). These stresses become lower than those of Ti-6Al-4V / aluminum oxide for k > 3.5 because the Al / Al2O3 reinforcing plate becomes richer in metal Al (lower stiffness: E$_{Al}$ < E$_{Ti-6Al-4V}$).

Figures 6, 7, 8 and 9 show the effect of the volume fraction of porosity on the normal and shear stresses as a function of the power index of a FGM beam in Al/ Al$_2$O$_3$ and Ti-6Al-4V/ Aluminum Oxide , respectively. The volume fraction of porosity is taken equal to 0.1, 0.15 and 0.2. The distribution shape of porosity in the FGM beam is considered uniform. It is clear that the effect of the volume fraction of porosity is greater when the FGM plate becomes richer in metal. The interface stresses are maximum when the FGM beam is stiffer (Al/Al$_2$O$_3$). The effect of

Fig. 6 Effect of the volume fraction of porosity on the normal stress of an Al/Al$_2$O$_3$ FGM beam reinforced in flexion with a porous varying properties plate under a uniformly distributed loading

porosity has less effect on the interfacial stresses when the reinforcing plate tends towards a non-homogeneous plate k = 4 and it has more effect when this plate tends towards a homogeneous plate (k tends to 0 or k tends to ∞).
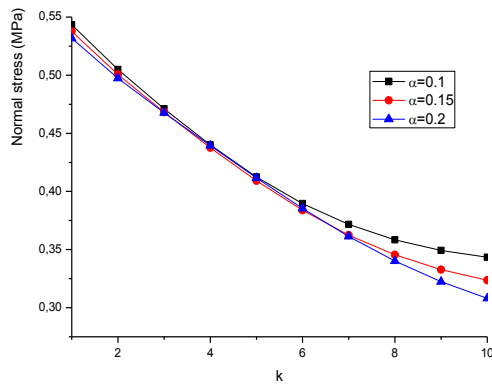
Fig. 7 Effect of the volume fraction of porosity on the normal stress of an Ti-6Al-4V/Aluminum Oxide FGM beam reinforced in flexion with a porous varying properties plate under a uniformly distributed loading
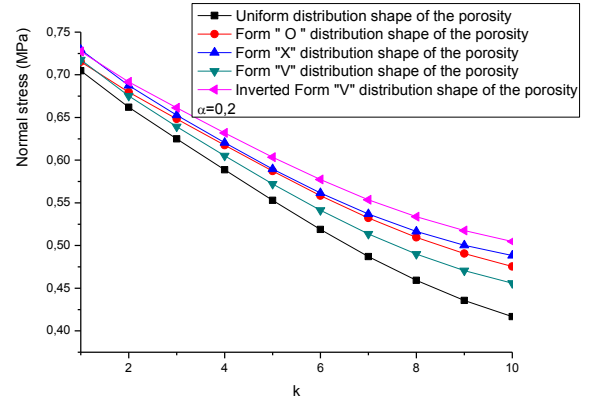

Fig 10. Effect of the porosity distribution form on the normal stress according to the power index of an Al/Al_2O_3 FGM beam reinforced in flexion with a porous varying properties plate under a uniformly distributed loading
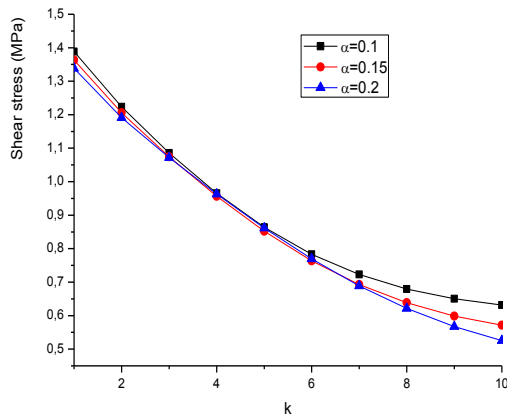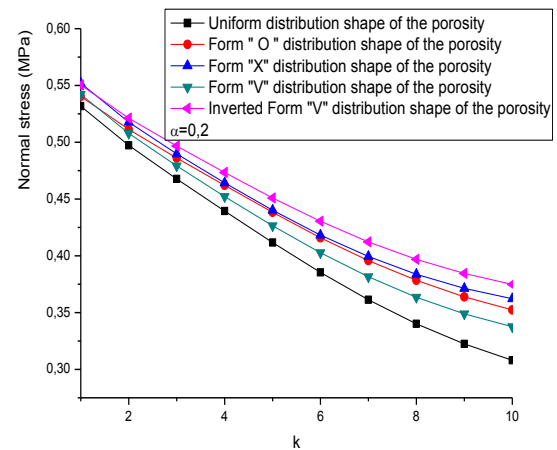

Fig. 8 Effect of the volume fraction of porosity on the shear stress of an Al/Al_2O_3 FGM beam reinforced in flexion with a porous varying properties plate under a uniformly distributed loading

Fig 11. Effect of the porosity distribution form on the normal stress according to the power index of an Ti-6Al-4V/Aluminum Oxide FGM beam reinforced in flexion with a porous varying properties plate under a uniformly distributed loading
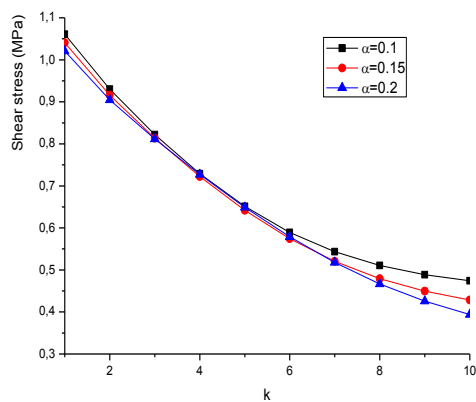

Fig. 9 Effect of the volume fraction of porosity on the shear stress of an Ti-6Al-4V/Aluminum Oxide FGM beam reinforced in flexion with a porous varying properties plate under a uniformly distributed loading

The influence of the porosity distribution shape as a function of the power index on the normal and shear stresses of a Al / Al_2O_3 and Ti-6Al-4V/ Aluminum Oxide FGM beam is illustrated in Figures 10, 11, 12 and 13, respectively. Various possible forms of porosity distribution have been considered. The volume fraction of porosity is taken equal to 0.2 (imperfect reinforcing plate). From these figures, the uniform distribution of the porosity leads to a significant reduction of the interface stresses because the reinforcing plates with an even distribution shape of porosity have a lower stiffness. These stresses become higher for inverted v-shaped distribution of porosity because the reinforcing plates with this distribution form of porosity have a higher stiffness.

The variation of the normal and shears stresses as a function of the thickness of the reinforcing plate of a Al/Al_2O_3 and Ti-6Al-4V/Aluminum Oxide FGM beam is shown in Figures 14, 15, 16 and 17, respectively. The load
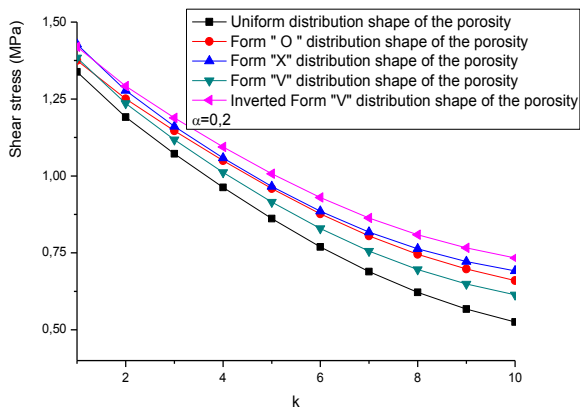
Fig 12. Effect of the porosity distribution form on the shear stress according to the power index of an Al/Al$_2$O$_3$ FGM beam reinforced in flexion with a porous varying properties plate under a uniformly distributed loading
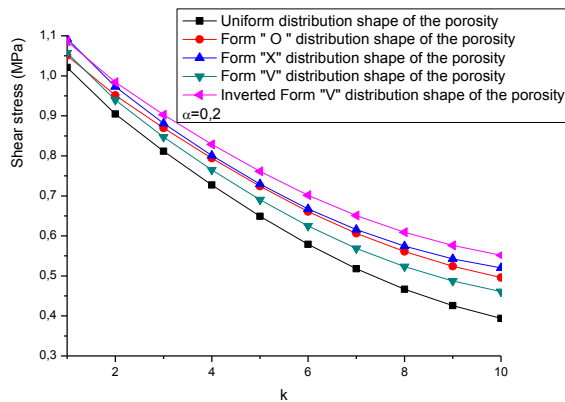

Fig 14. Effect of the porosity distribution form on the normal stress versus the thickness of the porous FGM plate of an Al/Al$_2$O$_3$ FGM beam under uniformly distributed loading

Fig 13. Effect of the porosity distribution form on the shear stress according to the power index of an Ti-6Al-4V/Aluminum Oxide FGM beam reinforced in flexion with a porous varying properties plate under a uniformly distributed loading

Fig 15. Effect of the porosity distribution form on the normal stress versus the thickness of the porous FGM plate of an Ti-6Al-4V/Aluminum Oxide FGM beam under uniformly distributed loading

is considered uniformly distributed. The reinforcing FGM plate is considered in (Al/Al$_2$O$_3$). The volume fraction of porosity is taken equal to 0.2 with different possible distribution forms. It is shown that the level and concentration of interfacial stress are influenced considerably by the thickness of the FG plate. Theinterfacial stresses increase as the thickness of FG plate increases (the plate becomes stiffer). This effect is similar to that of an increase in the plate elastic modulus shown in table 4 and Fig 10-13. For that it is strongly recommended to use a thinner plate thickness at the edges.

The variation of the normal and shears stresses as a function of the thickness of the adhesive layer of a Al /Al$_2$O$_3$ and Ti-6Al-4V / Aluminum Oxide FGM beam is shown in Figures 18, 19, 20 and 21, respectively. It is seen that increasing the thickness of the adhesive layer leads to significant reduction in the interfacial stresses. Thus using thick adhesive layer, especially in the vicinity of the edge, is recommended in order to avoid the peeling of the plate.
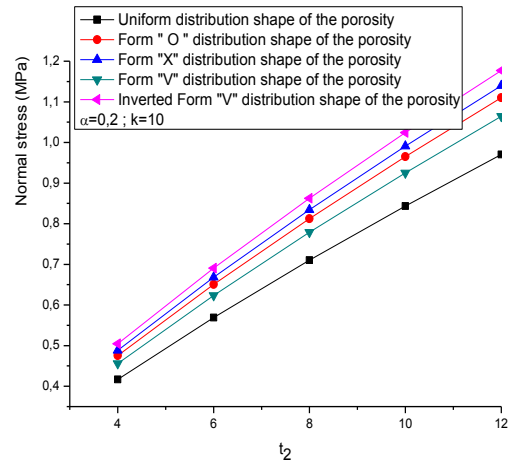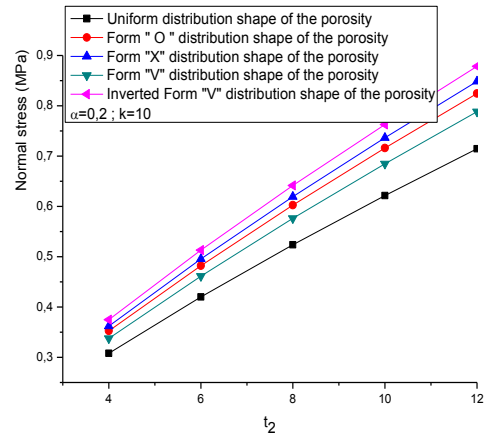

Fig 16. Effect of the porosity distribution form on the shear stress versus the thickness of the porous FGM plate of an Al/Al$_2$O$_3$ FGM beam under uniformly distributed loading

Fig 17. Effect of the porosity distribution form on the shear stress versus the thickness of the porous FGM plate of an Ti-6Al-4V/Aluminum Oxide FGM beam under uniformly distributed loading

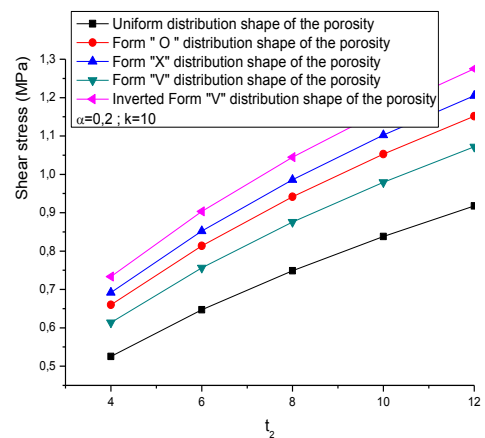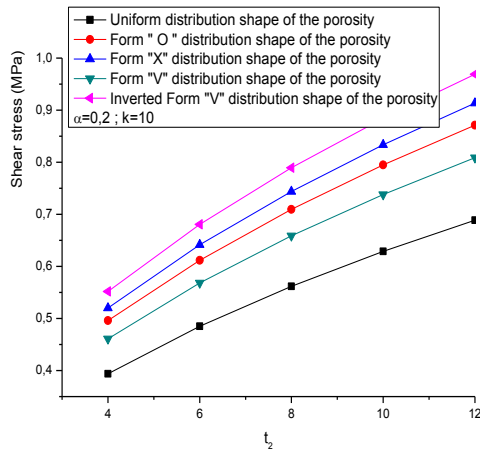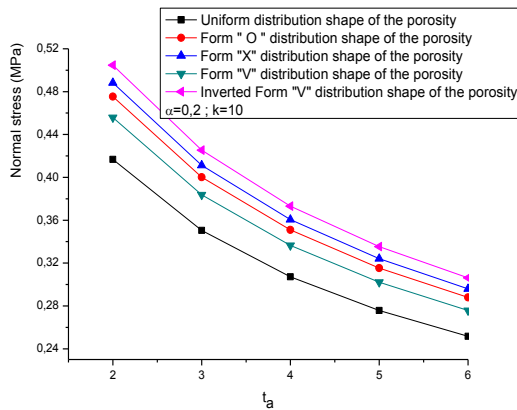Fig 20. Effect of the porosity distribution form on the shear stress as a function of the thickness of the adhesive layer of an Al/Al$_2$O$_3$ FGM beam reinforced with a porous FGM plate under uniformly distributed loading.

Fig 18. Effect of the porosity distribution form on the normal stress as a function of the thickness of the adhesive layer of an Al/Al$_2$O$_3$ FGM beam reinforced with a porous FGM plate under uniformly distributed loading.
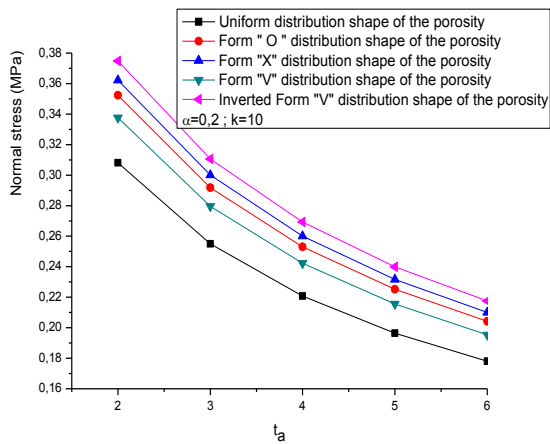

Fig 21. Effect of the porosity distribution form on the shear stress as a function of the thickness of the adhesive layer of an Ti-6Al-4V/Aluminum Oxide FGM beam reinforced with a porous FGM plate under uniformly distributed loading.
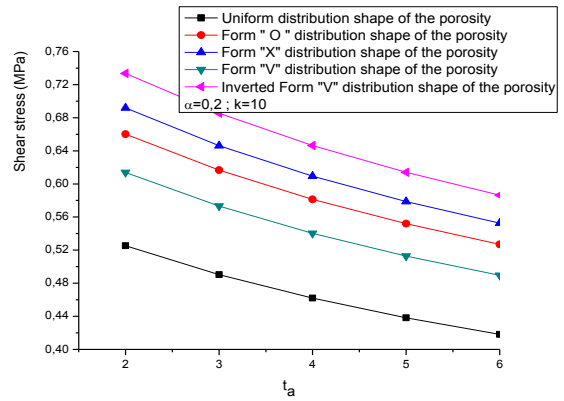
4. Conclusions

The effect of the porosity on the interfacial stresses has been presented for simply supported FG beams bonded with a porous FGM plate and subjected to a uniformly distributed load. Both even and uneven distribution shape of porosity are taken into account and the effective properties of FG plates with porosity are defined by theoretical formula with an additional term of porosity. The Poisson's ratio of the beam and the plate is assumed to be constant. The present study showed that interfacial stresses take a peak value when the reinforcement plate becomes richer in ceramic and diminished when the reinforcing plate contains porosity. In addition, as the power law index (*k*) increases, the effect of the distribution shape of porosity becomes more important. Another outcome based on the parametric study indicates that increasing the thickness of the adhesive layer reduces the stress concentration.
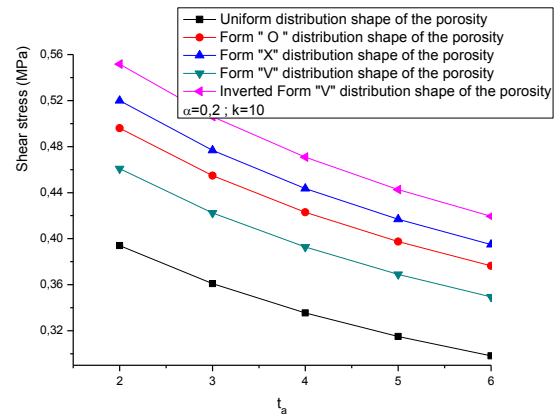

Fig 19. Effect of the porosity distribution form on the normal stress as a function of the thickness of the adhesive layer of an Ti-6Al-4V/Aluminum Oxide FGM beam reinforced with a porous FGM plate under uniformly distributed loading.

References

Rabahi, A., Adim, B., Chergui, S. and Hassaine Daouadji, T. (2015), "Interfacial stresses in FRP-plated RC beams: Effect of adherend shear deformations", *Multiphys. Model. Simulat. Syst. Des. Monit. Appl. Condition Monit.*, **2**, 317-326. https://doi.org/10.1016/j.ijadhadh.2008.06.008.

Abualnour, M., Houari, M.S.A., Tounsi, A. and Mahmoud, S.R. (2015), "Thermal buckling of functionally graded plates using a n-order four variable refined theory", *Adv. Mater. Res.*, **4**(1), 31-44. http://dx.doi.org/10.12989/amr.2015.4.1.31.

Abualnour, M., Houari, M.S.A., Tounsi, A. and Mahmoud, S.R. (2018), "A novel quasi-3D trigonometric plate theory for free vibration analysis of advanced composite plates", *Compos. Struct.*, **184**, 688-697. https://doi.org/10.1016/j.compstruct.2017.10.047.

Adim, B., Hassaine Daouadji, T. (2016) "Effects of thickness stretching in FGM plates using a quasi-3D higher order shear deformation theory", *Adv. Mater. Res.*, **5**(4), 223-244. https://doi.org/10.12989/amr.2016.5.4.223.

Adim, B., Hassaine Daouadji, T., Rabahi, A., Mohamed, B., Mohamed, Z. and Boussad, A. (2018), "Mechanical buckling analysis of hybrid laminated composite plates under different boundary conditions", *Struct. Eng. Mech.*, **66**(6),761-769. https://doi.org/10.12989/sem.2018.66.6.761.

Ait Atmane, H., Tounsi, A. and Bernard, F. (2015), "Effect of thickness stretching and porosity on mechanical response of a functionally graded beams resting on elastic foundations", *Int. J. Mech. Mater.*, 1-14. https://doi.org/10.1007/s10999-015-9318-x.

Al-Emrani, M. and Kliger, R. (2006), "Analysis of interfacial shear stresses in beams strengthened with bonded prestressed laminates", *J. Compos. Part B*, **37**, 265-272. https://doi.org/10.1016/j.compositesb.2006.01.004.

Arani, A.G., Mobarakeh, M.R., Shams, S. and Mohammadimehr, M. (2012), "The effect of CNT volume fraction on the magneto-thermo-electro-mechanical behavior of smart nanocomposite cylinder", *J. Mech. Sci. Technol.*, **26**(8), 2565-2572. https://doi.org/10.1007/s12206-012-0639-5.

Bakhadda, B., Bachir Bouiadjra, M., Bourada, F., Bousahla, A.A., Tounsi, A. and Mahmoud, S.R. (2018), "Dynamic and bending analysis of carbon nanotube-reinforced composite plates with elastic foundation", *Wind Struct.*, **27**(5), 311-324. https://doi.org/10.12989/was.2018.27.5.311.

Belabed, Z., Bousahla, A. A., Houari, M. S. A., Tounsi, A. and Mahmoud, S. R. (2018), "A new 3-unknown hyperbolic shear deformation theory for vibration of functionally graded sandwich plate", *Earthq. Struct.*, **14**(2), 103-115. https://doi.org/10.12989/eas.2018.14.2.103.

Bellifa, H., Bakora, A., Tounsi, A., Bousahla, A. A. and Mahmoud, S.R. (2017), "An efficient and simple four variable refined plate theory for buckling analysis of functionally graded plates", *Steel Compos. Struct.*, **25**(3), 257-270. https://doi.org/10.12989/scs.2017.25.3.257.

Rabia, B., Rabahi, A., Hassaine Daouadji, T., Abbes, B., Adim, B. and Abbes, F. (2018), "Analytical analysis of the interfacial shear

stress in RC beams strengthened with prestressed exponentially-varying properties plate", *Adv. Mater. Res.*, **7**(1), 29-44. https://doi.org/10.12989/amr.2018.7.1.029.

Rabia, B., Hassaine Daouadji, T., Hadji, L. and Mohamed Said Mansour (2016), "Static analysis of the FGM plate with porosities", *Steel Compos. Struct.*, **21**(1), 123-136. https://doi.org/10.12989/scs.2016.21.1.123.

Rabia, B., Hassaine Daouadji T. and Said Mansour, M. (2015), "A Higher Order Shear Deformation Model for Bending Analysis of Functionally Graded Plates", *Trans. Indian Inst. Met.*, **68**(1), 7-16. https://doi.org/10.1007/s12666-014-0428-1.

Rabia, B., Hassaine Daouadji, T. and Abderezak, R. (2019), "Effect of distribution shape of the porosity on the interfacial stresses of the FGM beam strengthened with FRP plate", *Earthq. Struct.*, **16**(5), 601-609. https://doi.org/10.12989/eas.2019.16.5.601.

Mohamed, B., Hassaine Daouadji, T., Abbes, B., Yu Ming Li, and Abbes, F. (2018), "Analytical and Numerical Results for Free Vibration of Laminated Composites Plates", *J. Chem. Molecul. Eng.*, **12**(6), 300-304.

Mohamed Amine, B., Hassaine Daouadji, T., Abbes, B., Adim, B., Yuming Li and Abbes, F. (2018a), "Dynamic analysis for anti-symmetric cross-ply and angle-ply laminates for simply supported thick hybrid rectangular plates" *Adv. Mater. Res.*, **7**(2), 83-103. https://doi.org/10.12989/amr.2018.7.2.119.

Bensattalah Tayeb, Mohamed Zidour and Hassaine Daouadji, T. (2018b), "Analytical analysis for the forced vibration of CNT surrounding elastic medium including thermal effect using nonlocal Euler-Bernoulli theory", *Adv. Mater. Res.*, **7**(3), 163-174. https://doi.org/10.12989/amr.2018.7.3.163.

Benhenni Mohamed Amine, Adim, B., Hassaine Daouadji, T., Abbes, B., Fazilay Abbes, Yuming Li and Ahmed Bouzidene (2019) "A comparison of closed form and finite element solutions for the free vibration of hybrid cross ply laminated plates", *Mech. Compos. Mater.*, **55**, 2. https://doi.org/10.1007/s11029-019-09803-2.

Benyoucef, S., Tounsi, A., Meftah, S.A. and Adda Bedia, E.A. (2006), "Approximate analysis of the interfacial stress concentrations in FRP-RC hybrid beams", *Compos Interfaces*, **13**(7), 561-571. https://doi.org/10.1163/156855406778440758.

Bouadi, A., Bousahla, A.A., Houari, M.S.A., Heireche, H. and Tounsi, A. (2018), "A new nonlocal HSDT for analysis of stability of single layer graphene sheet", *Adv. Nano Res.*, **6**(2), 147-162. https://doi.org/10.12989/anr.2018.6.2.147.

Bouakaz, K., Hassaine Daouadji, T., Meftah, S., Ameur, M. and Bedia, A. (2014), "A Numerical analysis of steel beams strengthened with composite materials", *Mech. Compos. Mater.*, **50**(4), 685-696. https://doi.org/10.1007/s11029-014-9435-x.

Bouhadra, A., Tounsi, A., Bousahla, A.A., Benyoucef, S. and Mahmoud, S.R. (2018), "Improved HSDT accounting for effect of thickness stretching in advanced composite plates", *Struct. Eng. Mech.*, **66**(1), 61-73. https://doi.org/10.12989/sem.2018.66.1.061.

Samir, B., Kerboua, B. and Bensaid, I. (2018), "Improved stresses analysis of a functionally graded beam under prestressed CFRP plate", *Adv. Compos. Lett.*, **27**(1), 10-22. https://doi.org/10.1177/096369351802700102.

Chaded, A., Hassaine Daouadji, T., Rabahi, A., Adim, B., Abbes, B., Benferhat, R. and Fazilay, A. (2018), "A high-order closed-form solution for interfacial stresses in externally sandwich FGM plated RC beams", *Adv. Mater. Res.*, **6**(6), 317-328. https://doi.org/10.12989/amr.2017.6.4.317.

Draiche, K., Tounsi, A. and Mahmoud, S.R. (2016), "A refined theory with stretching effect for the flexure analysis of laminated composite plates", *Geomech. Eng.*, **11**(5), 671-690. https://doi.org/10.12989/gae.2016.11.5.671.

El Mahi, K.H. Benrahou, K., Belakhdar, A. Tounsi, A. and Adda

Bedia, A. (2014), "Effect of the tapered of the end of a FRP plate on the interfacial stresses in a strengthened beam used in civil engineering applications", *Mech. Compos. Mater.*, **50**(4), 465-474. https://doi.org/10.1007/s11029-014-9433-z.

Farajpour, A., Yazdi, M.R.H., Rastgoo, A. and Mohammadi, M. (2016), "A higher-order nonlocal strain gradient plate model for buckling of orthotropic nanoplates in thermal environment", *Acta Mechanica*, **227**(7). https://doi.org/10.1007/s00707-016-1605-6.

Ghorbanpour Arani, A. and Haghparast, E. (2017), "Size-dependent vibration of axially moving viscoelastic micro-plates based on sinusoidal shear deformation theory", *J. Appl. Mech.*, **9**, https://doi.org/10.1142/S1758825117500260.

Guenaneche, B., Tounsi, A. and Adda Bedia, E.A. (2014), "Effect of shear deformation on interfacial stress analysis in plated beams under arbitrary loading", *Adhesion Adhesives*, **48**, 1-13. https://doi.org/10.1016/j.ijadhadh.2013.09.016.

Hassaine Daouadji, T. (2017) "Analytical and numerical modeling of interfacial stresses in beams bonded with a thin plate", *Adv. Comput. Design*, **2**(1), 57-69. https://doi.org/10.12989/acd.2017.2.1.057.

Hassaine Daouadji, T., Rabahi, A., Abbes, B., and Adim, B. (2016), "Theoretical and finite element studies of interfacial stresses in reinforced concrete beams strengthened by externally FRP laminates plate", *J. Adhesion Sci. Technol.*, **30**(12), 1253-1280. https://doi.org/10.1080/01694243.2016.1140703.

Hassaine Daouadji, T., Abdelaziz, H., Tounsi, A, and Adda, B. (2012), "A new Hyperbolic Shear Deformation Theory for Bending Analysis of Functionally Graded Plates", *Model. Simul. Eng.*, **10**, 1-10. https://doi.org/10.1016/j.apm.2014.10.045.

Hassaine Daouadji, T. (2013), "Analytical Analysis of the Interfacial Stress in Damaged Reinforced Concrete Beams Strengthened by Bonded Composite Plates", *Strength Mater.*, **45**(5), 587-597. https://doi.org/10.1007/s11223-013-9496-4.

Yang, J., Jianqiao, Ye and Zhongrong, N. (2007), "Interfacial shear stress in FRP-plated RC beams under symmetric loads", *Cement Concrete Compos.*, **29**(2007), 421-432. https://doi.org/10.1016/j.cemconcomp.2006.11.011.

Yang, J. and Jian Kao, Ye (2010), "An improved closed-form solution to interfacial stresses in plated beams using a two-stage approach", *J. Mech. Sci.*, **52**(2010), 13-30. https://doi.org/10.1016/j.ijmecsci.2009.09.041.

Kaci, A., Houari, M.S.A., Bousahla, A.A., Tounsi, A., Mahmoud, S.R. (2018), "Post-buckling analysis of shear-deformable composite beams using a novel simple two-unknown beam theory", *Struct. Eng. Mech.*, **65**(5), 621-631. https://doi.org/10.12989/sem.2018.65.5.621.

Khalifa, Z., Hadji, L., Hassaine Daouadji T. and Bourada, M. (2018), "Buckling response with stretching effect of carbon nanotube-reinforced composite beams resting on elastic foundation", *Struct. Eng. Mech.*, **67**(2), 125-130. https://doi.org/10.12989/sem.2018.67.2.125.

Khalifa Z., Hassaine Daouadji T., L. Hadji, Tounsi A, Adda bedia, (2016), "A New Higher Order Shear Deformation Model of Functionally Graded Beams Based on Neutral Surface Position", *Transac. Indian Institute Metals*, **69**(3), 683-691. https://doi.org/10.1007/s12666-015-0540-x.

Krour, B., Bernard, F. and Tounsi, A. (2014), "Fibers orientation optimization for concrete beam strengthened with a CFRP bonded plate: A coupled analytical-numerical investigation", *Eng. Struct.*, **9**, 218-227. https://doi.org/10.1016/j.engstruct.2013.05.008.

Mohammadimehr, M., Hooyeh, H.M., Afshari, H. and Salarkia, M.R. (2017), "Free vibration analysis of doublebonded isotropic piezoelectric Timoshenko micro-beam based on strain gradient and surface stress elasticity theories under initial stress using DQM", *Mech. Adv. Mater. Struct.*, **24**(4), 287-303.

https://doi.org/10.1080/15376494.2016.1142022.

Mohammadimehr, M., Mehrabi, M. and Hadizadeh, H. (2018b), "Surf ace and size dependent effects on static, buckling, and vibration of micro composite beam under thermomagnetic fields based on strain gradient theory", *Steel Compos. Struct.*, **26**(4), 513-531. https://doi.org/10.12989/scs.2018.26.4.513.

Mohammadimehr, M., Zarei, H.B., Parakandeh, A. and Arani, A.G. (2017b), "Vibration analysis of double-bonded sandwich microplates with nanocomposite facesheets reinforced by symmetric and un-symmetric distributions of nanotubes under multi physical fields", *Struct. Eng. Mech.*, **64**(3), 361-379. https://doi.org/10.12989/sem.2017.64.3.361.

Rabahi, A., Hassaine Daouadji, T., Abbes, B. and Adim, B. (2015), "Analytical and numerical solution of the interfacial stress in reinforced-concrete beams reinforced with bonded prestressed composite plate", *J. Reinforced Plastics Compos.*, **35**(3), 258-272. https://doi.org/10.1177/0731684415613633.

Rabahi A., Hassaine Daouadji, T., Benferhat R. and Adim B. (2018), "Elastic analysis of interfacial stress concentrations in CFRP-RC hybrid beams: Effect of creep and shrinkage", *Adv. Mater. Res.*, **6**(3), 257-278. ttps://doi.org/10.12989/amr.2017.6.3.257.

Rabahi A., Benferhat R., T. Hassaine Daouadji, B. Abbes, Adim B. and F. Abbes (2019), "Elastic analysis of interfacial stresses in prestressed PFGM-RC hybrid beams", *Adv. Mater. Res.*, **7**(2), 83-103. https://doi.org/10.12989/amr.2018.7.2.83.

Benferhat, R., Hassaine Daouadji, T., Mansour, Mohamed Said and Hadji, L. (2016), "Effect of porosity on the bending and free vibration response of functionally graded plates resting on Winkler-Pasternak foundations", *Eartq. Struct.*, **10**(5), 1429-1449. https://doi.org/10.12989/eas.2016.10.6.1429.

Shen, H.S., Teng, J.G. and Yang, J. (2001), "Interfacial stresses in beams and slabs bonded with thin plate", *J. Eng. Mech.*, **127**(4), 399-406. https://doi.org/10.1061/(ASCE)0733-9399(2001)127:4(399).

Smith, S.T. and Teng, J.G. (2001), "Interfacial stresses in plated beams", *Eng. Struct.*, **23**(7), 857-871. https://doi.org/10.1016/S0141-0296(00)00090-0.

Hassaine Daouadji, T., Abdelaziz H.H. and Adda bedia, E.A. (2013), "Elasticity Solution of a Cantilever Functionally Graded Beam", *Appl. Compos. Mater.*, **20**(1), 1-15. https://doi.org/10.1007/s10443-011-9243-6.

Hassaine Daouadji, T., Adim, B. and Benferhat, R., (2016), "Bending analysis of an imperfect FGM plates under hygro-thermo-mechanical loading with analytical validation", *Adv. Mater. Res.*, **5**(1), 35-53. http://dx.doi.org/10.12989/amr.2016.5.1.035.

Hassaine Daouadji, T. and Hadji, L. (2015), "Analytical solution of nonlinear cylindrical bending for functionally graded plates", *Geomech. Eng.*, **9**(5), 631-644. https://doi.org/10.12989/gae.2015.9.5.631.

Hassaine Daouadji, T., Tounsi A. and Adda Bedia, A. (2013), "Analyse et modélisation des poutres en béton armé renforcées par collage externe de plaques composites", *Revue des composites et des matériaux avancés*, **21**(2), 239-252.

Bensattalah, T., Zidour, M., Hassaine Daouadji, T. and Bouakaz, K. (2019), "Theoretical analysis of chirality and scale effects on critical buckling load of zigzag triple walled carbon nanotubes under axial compression embedded in polymeric matrix", *Struct. Eng. Mech.*, **70**(3), 269-277. https://doi.org/10.12989/sem.2019.70.3.269.

Touati, M., Tounsi, A. and Benguediab, M. (2015), "Effect of shear deformation on adhesive stresses in plated concrete beams: Analytical solutions", *Comput. Concrete*, **15**(3), 141-166. https://doi.org/10.12989/cac.2015.15.3.337.

Tounsi, A., Hassaine Daouadji, T., Benyoucef, S. and Adda Bedia, E.A. (2008), "Interfacial stresses in FRP-plated RC beams:

Effect of adherend shear deformations", *J. Adhesion Adhesives*, **29**, 313-351. https://doi.org/10.1016/j.ijadhadh.2008.06.008.

Tounsi, A. (2006), "Improved theoretical solution for interfacial stresses in concrete beams strengthened with FRP plate", *Int J Solids Struct*, **43**, 4154-4174. https://doi.org/10.1016/j.ijsolstr.2005.03.074.

Wattanasakulpong, N., Prusty, B. G., Kelly, D. W. and Hoffman, M. (2012), "Free vibration analysis of layered functionally graded beams with experimental validation", *Mater. Design*, **36**, 182-190. https://doi.org/10.1016/j.matdes.2011.10.049.

Wattanasakulpong, N. and Ungbhakorn, V. (2014), "Linear and nonlinear vibration analysis of elastically restrained ends FGM beams with porosities", *Aerosp. Sci. Technol.*, **32**(1), 111-120. https://doi.org/10.1016/j.ast.2013.12.002.

Yang, J. and Wu, Y.F. (2007), "Interfacial stresses of FRP strengthened concrete beams: Effect of shear deformation", *Compos. Struct.*, **80**, 343-351. https://doi.org/10.1016/j.compstruct.2006.05.016.

Zhu, J., Lai, Z., Yin, Z., Jeon, J. and Lee, S. (2001), "Fabrication of ZrO_2-NiCr functionally graded material by powder metallurgy", *Mater. Chem. Phys.*, **68**(1-3), 130-135. https://doi.org/10.1016/S0254-0584(00)00355-2.

Zidani, M.B., Belakhdar, K., Tounsi, A. and Adda Bedia, E.A. (2015), "Finite element analysis of initially damaged beams repaired with FRP plates", *Compos. Struct.* **134**, 429-439. https://doi.org/10.1016/j.compstruct.2015.07.124.

CC